DOI: 10.1007/s11099-014-0013-1 PHOTOSYNTHETICA 52 (1): 83-95, 2014

Molecular characteristics and expression patterns of Rubisco activase, novel alternative splicing variants in a heterophyllous aquatic plant, *Sagittaria graminea*

D. WANG[*,**,+], S.Z. XIE[#], J. YANG[***], and Q.F. WANG[*,**,+]

Key Laboratory of Aquatic Botany and Watershed Ecology, Chinese Academy of Sciences, Wuhan 430074, China[*]
Wuhan Botanical Garden, Chinese Academy of Sciences, Wuhan 430074, China[**]
School of Life Sciences, Fudan University, Shanghai 200433, China[***]
College of Science, Northwest A&F University, Yangling 712100, China[#]

Abstract

Two full-length cDNAs (SG*rca*1 and SG*rca*2) encoding ribulose-1,5-bisphosphate carboxylase/oxygenase (Rubisco) activase (RCA) were cloned from a heterophyllous aquatic plant, *Sagittaria graminea,* using Rapid-Amplification of cDNA Ends (RACE). SG*rca*1 contains a 1,320 bp open reading frame encoding a protein of 440 amino acids, and SG*rca*2 is exactly identical to SG*rca*1 except for 330 bp missing in the middle of SG*rca*1. Sequence analysis of cDNA and genomic DNA indicated both two cDNAs were generated from a common gene *via* alternative splicing. The deduced amino acid sequence encoded by SG*rca*1 showed 75–82% identity with other RCAs from higher plants and showed high homology in three highly conserved motifs associated with ATP-binding sites. RT-PCR analysis suggested both SG*rca*1 and SG*rca*2 were expressed in green tissues. During a 14 h light/10 h dark photoperiod, both aerial and submerged leaves exhibited the similar expression pattern of SG*rca*1 and SG*rca*2 with SG*rca*1 as the dominant form, but the accumulation of both SG*rca*1 and SG*rca*2 mRNA was significantly inhibited in the submerged leaves. Western blot analysis showed that both SG*rca*1 and SG*rca*2 had their translation products, the 43 kDa form and the 31 kDa form expressing in leaves. Interestingly, the aerial leaves expressed higher amount of the 43 kDa form compared with the 31 kDa form, while it was reversed in the submerged leaves. The results demonstrated that both environments regulated the RCA gene expression at both transcriptional and posttranscriptional level. In addition, co-immunoprecipitation assay revealed that the isolated Rubisco-RCA complex contained both the 43 and 31 kDa forms, and the proportion of the 31 kDa form was obviously enhanced in the submerged leaves. The results indicated that both the 43 kDa and 31 kDa forms were involved in Rubisco and RCA interaction and the increased incorporation of the 31 kDa form was associated with submerged photosynthetic environment.

Additional key words: Alismataceae; aquatic photosynthesis; heterophylly.

Introduction

RCA is required to maintain and regulate the activity of Rubisco in plants. It functions as a molecular chaperone (de Jiménez *et al*. 1995), catalyzing the activation of Rubisco *in vivo* by the ATP-dependent removal of various inhibitory sugar phosphates (Portis 2003). Plants expressing reduced levels of RCA exhibit the decrease of the net photosynthetic rate (P_N) and/or growth (Mate *et al*. 1996, Eckardt *et al*. 1997, He *et al*. 1997) and those with very low or no RCA expression can not survive in atmospheric CO_2 (Somerville *et al*. 1982, Salvucci *et al*. 1985, 1986; Mate *et al*. 1993, von Caemmerer *et al*. 2005). The gene expression and activity of RCA are thought to be the key regulation point for photosynthesis, especially under environmental stress (Crafts-Brandner and Salvucci 2000, Pollock *et al*. 2003, Portis 2003, Yamori *et al*. 2012). It makes the modulation of RCA an attractive experimental

Received 6 March 2013, *accepted* 24 July 2013.
[+]Corresponding authors; fax: +86-27-87510670, e-mail: qfwang@wbgcas.cn, dunwang@wbgcas.cn
Abbreviations: BTP – BIS-TRIS propane; DIG – digoxin; DTT – dithiothreitol; MCS – multiple clone site; ORF – open reading frame; P_N – net photosynthetic rate; PMSF – phenyl-methylsulfonyl fluoride; PVDF – polyvinylidene fluoride; PVPP – polyvinylpolypyrrolidone; qRT-PCR – quantitative real-time PCR; RACE – rapid-amplification of cDNA ends; RCA – Rubisco activase; Rubisco – ribulose-1,5-bisphosphate carboxylase/oxygenase; RT-PCR – reverse transcription PCR; UTR – untranslated region.
Acknowledgements: This work was supported by grants from National Natural Science Foundation of China (31100162, 30970202) and Strategic Pilot Science and Technology Projects of the Chinese Academy of Sciences (XDAO5090305).

goal for the study of photosynthetic carbon assimilation.

RCA belongs to the protein family of ATPases, associated with diverse cellular activities (AAA^+ family), and it contains the common AAA motifs that characterize the family members, including Walk A, Walk B, and nucleotide sensor domains (Neuwald *et al*. 1999, Portis 2003). RCA is a nuclear-encoded, chloroplast enzyme, usually present in two isoforms (α- and β-isoform, with molecular masses of 45–48 kDa and 41–43 kDa, respectively) in most species studied (Salvucci *et al*. 1987, Portis 2003). In plants, such as spinach (Werneke *et al*. 1988), *Arabidopsis* (Werneke *et al*. 1988), barley (*rcaA* gene, Rundle and Zielinski 1991), and rice (To *et al*. 1999, Zhang and Komatsu 2000), alternative splicing of one RCA pre-mRNA results in two isoforms of RCA, differing only at the C-terminus. However, in other species, the RCA genes are not alternatively spliced. For example, the RCA α- and β-isoform are encoded by two different genes in cotton (Salvucci *et al*. 2003), and another RCA gene (*rcaB*) in barley encodes only the β-isoform of RCA. Furthermore, sequence analysis of RCA cDNAs suggested that it might be only the β-isoform in tobacco, maize, bean, cucumber, and mung bean (Portis 2003). *In vitro* experiments have shown that both α- and β-isoform are capable of promoting Rubisco activation but they differ markedly in their enzyme activity (Shen *et al*. 1991). Subsequent studies demonstrated that light regulation of RCA activity was achieved by the redox regulation of the α-isoform *via* thioredoxin-f (Zhang and Portis 1999, Zhang *et al*. 2002). Studies in some plants also showed that the alternative isoforms of RCA have been shown to be differentially sensitive to thermal denaturation. Variations in the expression of the isoforms may play a role in photosynthetic acclimation to high temperature in these species (Crafts-Brandner *et al*. 1997, Law and Crafts-Brandner 2001, Law *et al*. 2001, Wang *et al*. 2010). Taken together, the functional difference and expressional diversity of the different RCA forms suggest RCA proteins play the important role in photosynthetic adaptation to different environments.

Compared to terrestrial plants, little information noccerning RCA is reported in aquatic plants. Development of heterophylly is one of the ways how aquatic plants adapt to aerial and submerged environments. *S. graminea* is the typical, heterophyllous plant that grows in aqueous habitats. This amphibious plant bears linear, submerged leaves that utilize water-dissolved inorganic carbon, and also ovoid, aerial leaves that use atmospheric CO_2. The submerged leaves are the first to develop out of a seed or a dormant rhizome in the spring. As the emerging leaves grow, they comprise the main photosynthetic biomass during most of the growing season. There are remarkable differences between the atmospheric and submerged conditions in light intensity, CO_2 concentration, and temperature. This raises the question how *rca* genes from both leaf types are expressed and regulated to adapt to such different conditions. To answer this question, we cloned and sequenced the cDNAs and genomic DNA encoding RCA protein from *S. graminea* plant and sought to compare the gene expression pattern of RCA between the aerial and submerged leaf types at both mRNA and protein levels.

Materials and methods

Plant material and culture condition: The plants of *S. graminea* (Alismataceae) were grown in the aquatic-plant pond in Wuhan Botanical Garden, Chinese Academy of Sciences. Aerial and submerged leaf tissues used for RNA and protein experiments were sampled from seedlings with 2–3 aerial leaves using liquid N_2, and stored at –80ºC.

Cloning of full-length RCA cDNA by RACE from *S. graminea*: Total RNA from each sample was extracted using the *TaKaRa* RNAiso plus reagent (Dalian, China), and treated with RNase-free DNase I (*TaKaRa*, Dalian, China) according to the manufacturer's instructions. The concentration of total RNA was determined *via* optical density measurement (*DU730*, *Beckman*, Germany). 5'- or 3'-RACE-Ready cDNA was synthesized from 1 μg total RNA using *BD SMART™ RACE cDNA Amplification Kit* (*Clontech*, Palo Alto, USA) according to the manufacturer's instructions. Full-length RCA cDNAs were cloned in three steps: (*1*) cloning of specific fragment; (*2*) cloning of 5'- and 3'- cDNA ends; (*3*) cloning of full-length RCA cDNA. The specific fragment of RCA cDNA was amplified using a primer pair of CF-F and CF-R (Table 1), which were designed in the conserved regions of the corresponding genes from Viridiplantae. PCR conditions: 1 cycle of 94ºC for 3 min; 30 cycles of 94ºC for 30 s, 60ºC for 30 s, and 72ºC for 1 min; with final extension step of 72ºC for 10 min. After electrophoresis in a 0.8% agarose gel, the PCR product was purified using the *SanPrep Gel Purification Kit* (*Sangog*, Shanghai, China), and then TA-cloned into pMD19-T vectors using a *pMD® 19-T simple Vector Kit* (*TaKaRa*, Dalian, China) followed by sequencing. According to the sequence of specific fragment, a pair of gene-specific primers (5-GSP for 5'RACE, and 3-GSP for 3'-RACE; Table 1) and a pair of nested gene-specific primers (5-nGSP for 5'RACE, and 3-nGSP for 3'-RACE; Table 1) were designed for amplification of the 5'- and 3'- fragments according to the manufacturer's instructions of the *BD SMART™ RACE cDNA Amplification Kit* (*Clontech*, Palo Alto, USA). After aligning and assembling the 5'- and 3'- fragments, the full-length cDNA sequence was deduced, and further confirmed by PCR using a pair of full-length primer (RCA-F,

Table 1. Primers designed for *rca* gene cloning and qRT-PCR analysis.

Primer ID	Sequences	Purpose
CF-F	5'–TTCATGGACAAGCTYGTYGTYCAC-3'	Conserved fragments cloning
CF-R	5'–GCCCAGTAGAACTTCTCCAT-3'	
5-GSP	5'–GTTCATGGACAAGCTGGTCGTCCAC-3'	5' RACE PCR
5-nGSP	5'–AAATCCTTCCAGTGTGAGCTCGT-3'	
3-GSP	5'–GCCCAGTAGAACTTCTCCATACG-3'	3' RACE PCR
3-nGSP	5'–GTGGCGTTCACCATCTGGTTGTT-3'	
RCA-F	5'–ATCAGCTAGGTGGTTGAGCAGTT-3'	Full length cloning
RCA-R	5'–GGTTCTCTTCCGAGGTTGCA-3'	
RT-1-F	5'–ACAAGCTGGTCGTCCACATCGCTAA-3'	Real Time qPCR for SG*rca*1
RT-1-R	5'–AGCTCTCCGGCGCTCATCATG-3'	
RT-2-F	5'–CCCAACATCAAGCTCCCAGGG-3'	Real Time qPCR for SG*rca*2
RT-2-R	5'–CTGCTCGGGTACGTTGTCGGC-3'	
actin-F	5'–AAGTCCTCTTCCAGCCCTCGCTCA-3'	Real Time qPCR for β-actin
actin-R	5'–GCAATACCCGGGAACATGGTTGTC-3'	
DIG-F	5'–ATCAGCTAGGTGGTTGAGCAG-3'	Probe labeling
DIG-R	5'–GTTGACATAGTCAATTAAGATAGATAGC-3'	

RCA-R; Table 1). PCR was performed as follows: 1 cycle of 94ºC for 3 min, 35 cycles of 94ºC for 45 s, 60ºC for 30 s, 72ºC for 2 min, and 1 cycle at 72ºC for 10 min.

Cloning of genomic *rca* coding gene from *S. graminea*: Genomic DNA was isolated using a *Plant Genomic DNA isolation Kit* (*Sangog*, Shanghai, China). Using the full-length primers (RCA-F/R; Table 1), the genomic RCA DNA was amplified by PCR with the genomic DNA as template. PCR using LA-Taq DNA polymerase (*TaKaRa*, Dalian, China) was performed as follows: 1 cycle of 94ºC for 5 min, 30 cycles of 98ºC for 15 s, 60ºC for 30 s, 72ºC for 5 min, and 1 cycle at 72ºC for 10 min.

Southern hybridization: Genomic DNA (20 μg) of *S. graminea* was digested with *BamH I*, *EcoR I* or *Bgl I* separately. After electrophoresis in a 0.8% agarose gel, the digested DNA fragments were transferred onto a nitrocellulose membrane (*Roche*, Germany). The DIG-F and DIG-R primers (Table 1), which were used to synthesize DIG-labeled probes, were designed based on the 500 bp fragment at 5'-end of genomic *S. graminea rca* gene. Specific *rca* probe labeling, blot hybridization, and immunodetection were performed using a *DIG High Prime DNA Labeling and Detection Starter Kit I* (*Roche*, Germany) according to the manufacturer's instructions.

Bioinformatics analysis and phylogenetic tree construction: The nucleotide sequence, deduced amino acid sequence, and open reading frame (ORF) were analyzed using *DNAstar* software, and the sequence comparison was conducted through a database search using *BLAST*. The *S. graminea* RCA amino acid sequence and other RCA amino acid sequences retrieved from NCBI were aligned using *ClustalX*, and then a phylogenetic tree was constructed using neighbor-joining method with the software *MEGA5*, and the bootstrap test was carried out with 1,000 iterations. Chloroplast transit peptide was predicted by *ChloroP 1.1* Server network analysis (http://www.cbs.dtu.dk/services/ChloroP/).

Semiquantitative RT-PCR and quantitative real-time PCR (qRT-PCR): Tissues-specific expression of *rca* coding gene was determined by semi-quantitative RT-CR. Total RNA was isolated from root, flower, sepal, aerial and submerged leaf using the *TaKaRa* RNAiso plus reagent (Dalian, China). For each sample, 1 μg DNase I-treated total RNA was used for first-strand cDNA synthesis using an oligo(dT) primer and PrimeScript reverse transcriptase (*TaKaRa*, Dalian, China) according to the supplier's manual. One μl of cDNA was used as the template for a 50 μl PCR amplification with full length primers (RCA-F/RCA-R, Table 1). Actin was used as an internal standard (actin-F/R, Table 1). PCR was performed as follows: 1 cycle of 94ºC for 3 min, 22 cycles of 94ºC for 45 s, 60ºC for 30 s, 72ºC for 2 min, and 1 cycle at 72ºC for 10 min.

Steady-state mRNA expression analyses of SG*rca*1 and SG*rca*2 were carried out by quantitative real-time PCR (qRT-PCR). Total RNA was isolated from the aerial and submerged leaves, which were sampled every 3 h during a 24-h time course (14 h light/10 h dark). For each sample, 2 μg DNase I-treated total RNA was used for first-strand cDNA synthesis using random hexamer primers and a *PrimeScript® RT reagent kit* (*TaKaRa*, Dalian, China). First-strand cDNA was diluted for 1:30 with nuclease-free water prior to qRT-PCR. A pair of SG*rca*1-specific přimers (RT-1-F/R, Table 1) located in the characteristic exon of SG*rca*1, and a pair of SG*rca*2-specific primers (RT-2-F/R, Table 1) covered the predicted alternative spliced sites were designed for quantitative analysis of the two transcripts. Reaction specificity for each primer pair was tested using PCR amplification of cDNA, electrophoresis gels, cloning and sequencing of each plasmid, and melting curve analysis. β-actin was chosen as a reference gene.

qRT-PCR was carried out on an *Applied Biosystems StepOne Real-Time PCR System* (*Life Technologies Co.*, Carlsbad, USA) using the comparative CT method. All reactions were measured in triplicate, using 2× *SYBR® Premix Ex Taq™* (*TaKaRa*, Dalian, China). The amplification program was performed as follows: 95ºC for 30 s, 40 cycles of 95ºC for 5 s, 63ºC for 30 s.

Leaf protein extraction and Western blot analysis: About 0.2 g of frozen leaves were ground to a fine powder with liquid N_2 using mortar and pestle, a small amount of quartz sand, and insoluble polyvinyl-polypyrrolidone (PVPP). Then the samples were homogenized with 1 ml of cooled extraction buffer at 0–4ºC. The extraction buffer contained 10 mM BIS-TRIS propane (BTP), pH 7.0, 5 mM $MgCl_2$, 1 mM EDTA, 0.4 mM ATP, 15 mM DTT, 1 mM phenyl-methylsulfonyl fluoride (PMSF), 2 mM benzamidine, and 0.01 mM leupetine. The homogenate was centrifuged at 15,000 × *g* for 10 min at 4ºC. The supernatant was used to determine the amount of total protein using Coomassie Brilliant Blue method (Bradford, 1976). The equal amount of total proteins from each sample was separated by SDS-PAGE and transferred to a polyvinylidene fluoride (PVDF) membrane. Blots were probed with monoclonal antibody against rice RCA (Wang *et al*. 2009) and visualized using alkaline phosphatase conjugated to a secondary antibody.

Co-immunoprecipitation assay: Total soluble proteins from the aerial or submerged leaf samples were isolated rapidly with extraction buffer as described above, except that 5 mM ATP was included in the extraction buffer. The Rubisco-RCA complex was isolated from the leaf extracts with antibody against rice Rubisco large subunit as described previously (Wang *et al*. 2010). The isolated Rubisco–RCA complex was separated by SDS-PAGE and transferred to the PVDF membrane, followed by immunoblot analysis using the monoclonal antibody against rice RCA.

Results

Cloning and sequence analysis of full-length cDNAs from *S. graminea* leaves: The 5' and 3'-cDNA ends of *rca* from *S. graminea* were cloned by RACE PCR to explore the *rca* coding gene. Full-length cDNA of *S. graminea rca* was reconstructed by joining the sequences of a single 5'-end and 3'-end. The sequence of full-length cDNA was further confirmed by full-length amplification using a pair of primer (SG-full-F/ SG-full-R, Table 1), which were designed in 5'- and 3'-untranslated region (UTR). Sequencing of 50 random clones revealed two different cDNA clones produced by full-length PCR. The longer one was 1,631 bp (designated as SG*rca*1, GeneBank accession number KC678993), and the short one was 1,301 bp (designated as SG*rca*2, GeneBank accession number KC678994). SG*rca*1 had an 1,320 bp open reading frame encoding a polypeptide of 440 amino acids with the calculated molecular mass of 48.2 kDa and the isoelectric point of 7.824. SG*rca*2 had an 990 bp open reading frame encoding a polypeptide of 330 amino acids with the calculated molecular mass of 36.4 kDa and the isoelectric point of 6.623. Sequence alignment suggested that SG*rca*2 was exactly identical to SG*rca*1 except for 330 bp missing in the middle of SG*rca*1 (571–900 bp, Fig. 1), which was 110 amino acids shorter than SG*rca*1. The identical 5'-UTR was 114 bp upstream of the translation start codon ATG and the identical 3'-UTR was 193 bp downstream from the stop codon. The two cDNA clones shared the common sequence of 5'- and 3'-UTR indicating that both cDNAs represented mRNAs transcribed from the common gene. *ChloroP 1.1 Server* network analysis indicated that about 55 amino acids at the N-terminal of both clones constitute a putative chloroplast transit peptide. Cutting off the chloroplast transit peptide, the transcripts of SG*rca*1 and SG*rca*2 encode 43 and 31 kDa mature proteins, respectively.

Cloning and sequencing of *S. graminea rca* genomic clone: Sequencing of 30 random genomic *rca* DNA clones revealed only one gene type was obtained. This genomic amplification product was 1,748 bp and it was designated as SG*rca* (GeneBank accession number KC553979). The PCR amplification products of full-length primer using cDNA or genomic DNA as template were compared through gel electrophoresis (Fig. 2). Two amplification products (confirmed by sequencing as SG*rca*1 and SG*rca*2, respectively) from cDNA template and only one amplification product (SG*rca*) from the genomic DNA template supported the conclusion that both two transcripts were generated from one gene *via* alternative splicing. Gene structure analysis was performed by comparing the genomic sequence and cDNA sequence. SG*rca* was composed of two introns and three exons (Fig. 3). Compared with SG*rca*1, SG*rca*2 had 171 bp missing at the 3'-end of exon 2 and 159 bp missing at the 5'-end of exon 3, which suggested that both two mRNA could be generated from the common gene by reserving or discarding 171 bp at the 3'-end of exon 2 and 159 bp at the 5'-end of exon 3.

Genome analysis: The *S. graminea* genomic blot (Fig. 4) was probed with a specific probe containing the 5'-end region (501 bp) of genomic *rca* clone in order to estimate the copy number of the gene. No *BamH I* or *EcoR I* sites

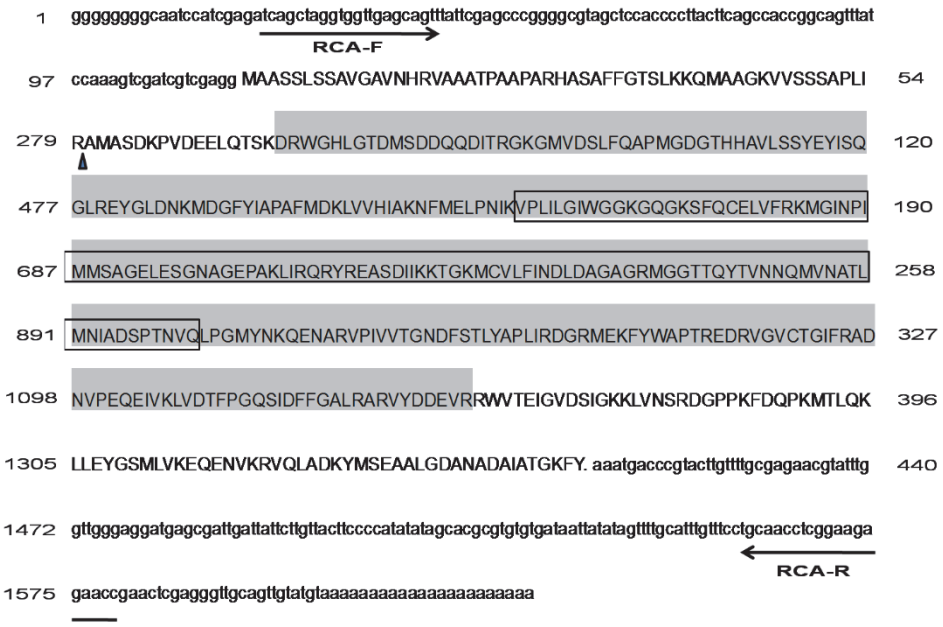

Fig. 1. The nucleotide and deduced amino acid sequence of SG*rca*1 and SG*rca*2. The number of nucleotide sequence is on the left and the number of deduced amino acid sequence is on the right. The high conserved P-loop NTPase Super family domain is marked with *gray background*. The 330 bp fragment missing in SG*rca*2 is indicated with *black frame*. The cleavage site of putative chloroplast transit peptide is indicated by *triangle*. The *horizontal arrows* show the full length primers RCA-F/R.

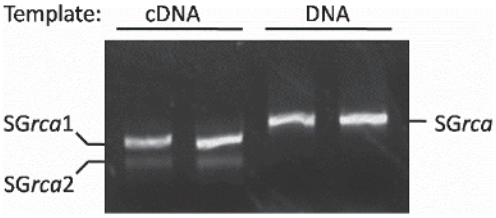

Fig. 2. Amplification products of *rca* gene using cDNA (two panels on the left) or genomic DNA (two panels on the right) as templates. PCRs were performed using full-length primer pair RCA-F/R (Table 1).

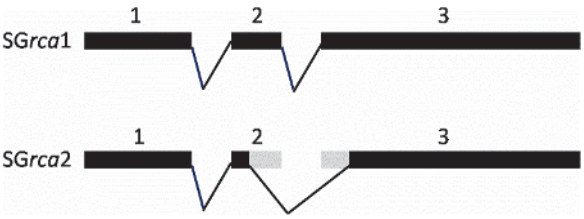

Fig. 3. Gene structure of SG*rca*1 and SG*rca*2 cDNA. *Black bars* indicate the exons and *gray bars* indicate the missing fragments in SG*rca*2. Splicing patterns were indicated by *fold lines*.

were found in the *rca* genomic clone. A single band hybridized specifically to the *rca* probe was observed when genomic DNA was digested with *BamH I* or *EcoR I*. One restriction site for *Bgl I* was found in the genomic *rca* clone. Two bands hybridized specifically to the *rca* probe were observed upon *Bgl I* digestion of the genomic DNA. Taken together, these results indicated that there was only one *rca* gene per genome in *S. graminea*.

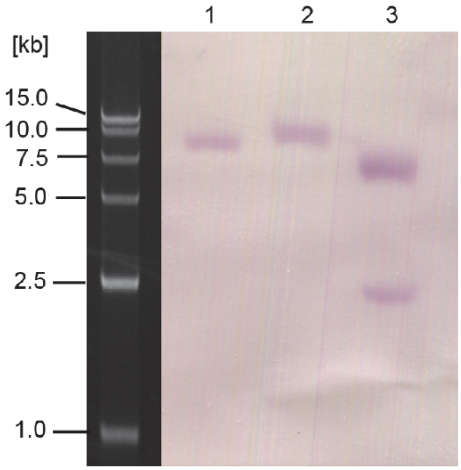

Fig. 4. Genomic Southern blot analysis of the *rca* gene. *Sagittaria graminea* genomic DNA was digested completely with *BamH I* (*lane 1*), *EcoR I* (*lane 2*) or *Bgl I* (*lane 3*) separately, separated by 0.8% agarose electrophoresis, and then blotted onto a nitrocellulose membrane. The blot was hybridized to a 501 bp specific DIG-labeling probe. Molecular size markers are indicated on the left.

Bioinformatics analysis of SG*rca*1 and SG*rca*2 encoding proteins: Multiple alignment analysis was performed using RCA protein sequence from 9 different plant species. Homology analysis showed that the protein encoded by SG*rca*1 shared 75–82% homology to RCAs from higher plants. Conserved motifs and critical residues associated with enzyme activity were marked in Fig. 5.

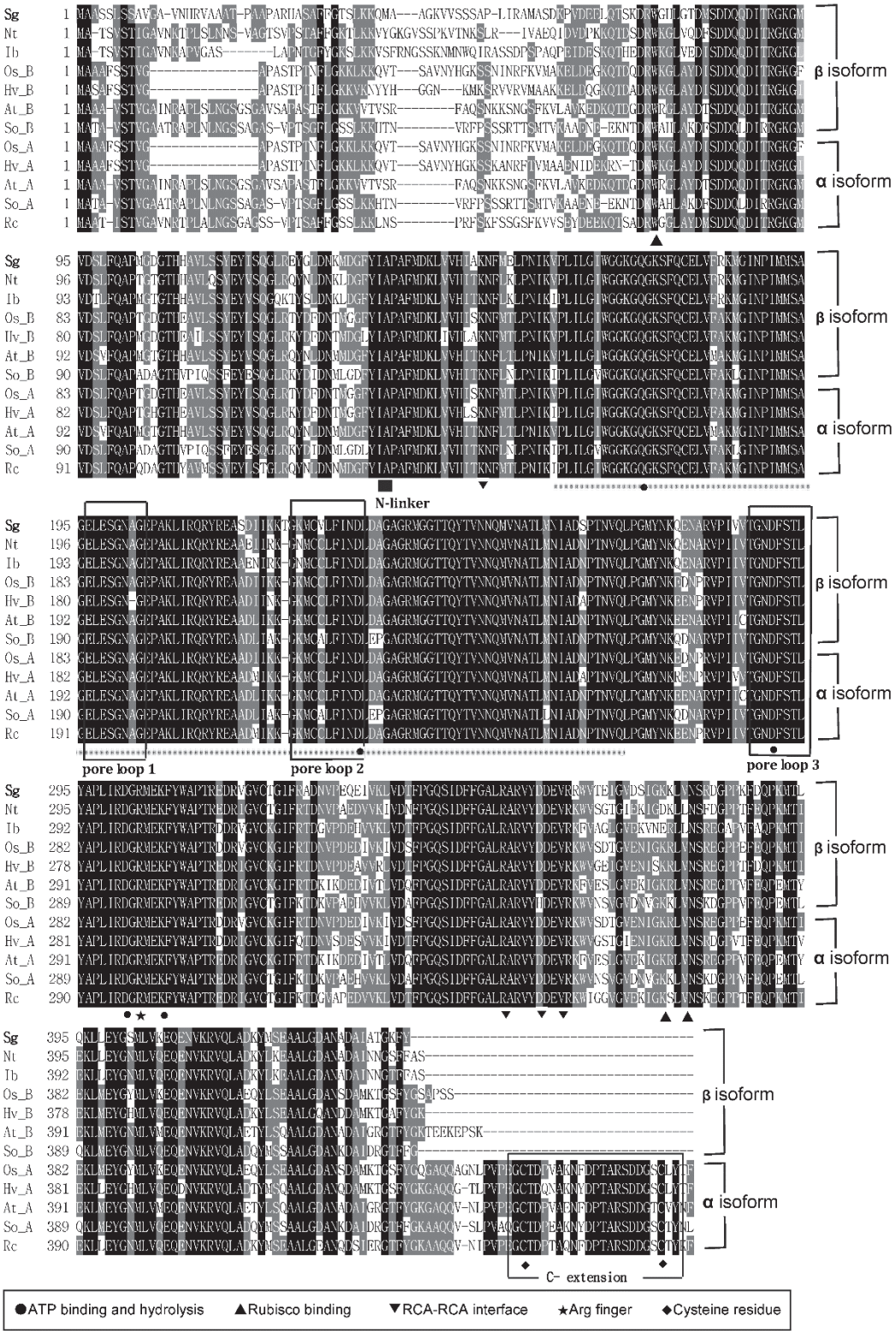

Fig. 5. Alignment of representative RCA sequences. Multiple alignment of the amino acid sequence of RCA among *Sagittaria graminea* (Sg), *Nicotiana tabacum* (Nt), *Impomea batatas* (Ib), *Oryza sativa* (Os), *Hordeum vulgare* (Hv), *Arabidopsis thaliana* (At), *Spinacia oleracea* (So), and *Ricinus communis* (Rc) were performed using *Clustal-X*. In the alignment, similar residues are shown in *gray* and identical residues in *black background*. *Gray bar* indicates the missing amino acid residues in SG*rca*2. *Black bar* indicates the instable N-linker. Symbols below the sequence indicate highly conserved key amino acid residues associated with representative functions. Three pore loop motifs essential for ATP binding and hydrolysis, and C-extension of RCA α isoform are indicated with *black frames*.

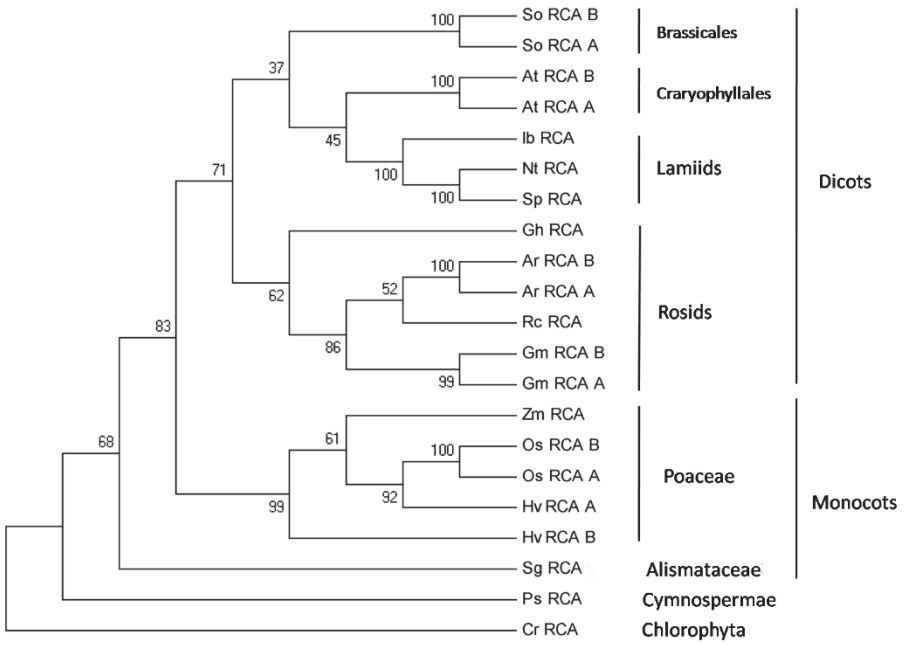

Fig. 6. Phylogenetic tree of RCAs from various species. Multiple alignment of the amino acid sequence of RCA among *Spinacia oleracea* (So), *Arabidopsis thaliana* (At), *Impomea batatas* (Ib), *Nicotiana tabacum* (Nt), *Solanum pennellii* (Sp), *Gossypium hirsutum* (Gh), *Acer rubrum* (Ar), *Ricinus communis* (Rc), *Glycine max* (Gm), *Zea mays* (Zm), *Oryza sativa* (Os), *Hordeum vulgare* (Hv), *Sagittaria graminea* (Sg), *Picea sitchensis* (Ps), and *Chlamydomonas reinhardtii* (Cr) were performed using *Clustal-X*. Phylogenetic tree was constructed using neighbor-joining method with the software *MEGA 5*.

The putative amino acid sequence of SG*rca*1 contained three pore loop motifs (GGKGQGKS, Loop 1; GNMCCLFIND, Loop 2; TGNDFSTL, Loop 3), which are essential for ATP binding and hydrolysis. However, the absense of 110 amino acids in the amino acid sequence of SG*rca*2 resulted in two of the three pore loop motifs missing (pore loop 1 and pore loop 2). It has been demonstrated that mutation of several critical residues in pore loop 1 or pore loop 2 would led to the function loss of ATPase activity (Stotz *et al*. 2011). The entire missing of pore loop 1 and pore loop 2 likely causes the loss of the ATPase functions. However, SG*rca*2 still reserved some highly conserved motifs containing critical residues that are associated with Rubisco binding (residue 74, 375, and 378) and RCA subunit interaction (residue 150, 353, 358, and 361). In addition, both SG*rca*1 and SG*rca*2 do not encode both of the critical cysteine residues that would be required for redox regulation by α isoform (Zhang *et al*. 2002, Zhang and Portis 1999), suggesting that two proteins encoded by SG*rca*1 and SG*rca*2 belong to β isoform (Fig. 5). Phylogenetic tree was constructed using the entire RCA amino acid sequence by neighbor-joining method. As shown in Fig. 6, SG*rca*1 is in the base of angiosperm group, and it is closely related to gymnospermous *Picea sitchensis* in accordance with its taxonomic status.

Expression of RCA protein in aerial and submerged leaves of *S. graminea*: To investigate the RCA protein expression in different leaf types of *S. graminea*, a specific monoclonal antibody (MAb, Wang *et al*. 2009) against rice RCA was used for Western blot assay (Fig. 7). *Arabidopsis* and spinach leaves were used as a positive control. Two RCA isoforms with molecular mass of 41–45 kDa were recognized in leaf extracts from *Arabidopsis* and spinach, respectively, indicating that the used MAb had a good specificity to RCA proteins from different plants. Both in the aerial and submerged leaves of S. *graminea*, two RCA polypeptides were detected, the longer one with molecular mass about 43 kDa and the shorter one with a molecular mass about 31 kDa (Fig. 7*A*). The densitometric analysis of protein bands (Fig. 7*B*) showed that the 43/41 kDa RCA ratio of the aerial leaf was 1.818 ± 0.421 (n = 3), while that of the submerged leaf was 0.591 ± 0.111 (n = 3). Hence, the 43 kDa RCA was the dominant form in the aerial leaves, whereas it was reversed in the submerged leaves.

It was reported that the N terminal of RCA seemed to be unstable and likely to be cleaved proteolytically at the site of N-linker (Fig. 5). This might lead to a proteolytic product that should have the similar molecular mass with the polypeptide encoded by SG*rca*2. The proteolytic product should contain 110 amino acids (110 AA) that were absent in SG*rca*2 coding protein. To clarify whether the detected 31 kDa isoform was the proteolytic product or the expressed protein encoded by SG*rca*2, a fusion protein (Fig. 8*A*) containing 110 AA was expressed in *E. coli* BL21 (DE3) cells. Then it was used as the antigen to

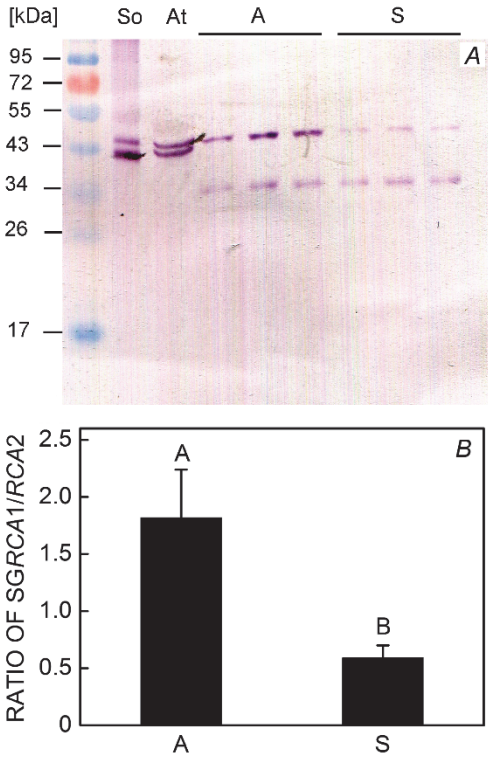

Fig. 7. Western blotting analysis of the Rubsico activase from *S. graminea* leaves. *A*: Leaf tissues from aerial (A) and submerged (S) leaf of *S. graminea* were extracted in buffer, and the crude extracts (8 μg total protein) were separated by SDS-PAGE and transferred to a PVDF membrane. Blots were probed with monoclonal antibody against rice RCA and visualized using alkaline phosphatase conjugated to a secondary antibody. Samples (4 μg total protein) from *Spinacia oleracea* (So) and *Arabidopsis thaliana* (At) leaf were used as control. *B*: The densitometric analysis of protein bands was performed with *Quantity One* software, and the calculated ratios of SG*rca*1/*rca*2 from different tissues were shown. Symbols marked with *the same letters* were not significantly different ($p<0.05$) for different samples. The results presented are the means ± SD ($n = 3$).

produce specific polyclonal antibody (Fig. 8*B*). After affinity purification with MAb against RCA mentioned above, the two RCA isoforms from *S. graminea* leaf extract were separated by SDS-PAGE and probed with the polyclonal antibody anti-110 AA. As shown in Fig. 8*C*, this polyclonal antibody could only recognize the 43 kDa isoform but not the 31 kDa isoform, suggesting that the 31 kDa protein did not contain the 110 AA. Hence, the 31 kDa protein should not be the proteolytic product of the 43 kDa form. These results demonstrated that both SG*rca*1 and SG*rca*2 had their translation products in *S. graminea* leaves.

Accumulation patterns of SG*rca*1 and SG*rca*2 mRNA: To determine the tissue expression pattern of SG*rca*1 and SG*rca*2, their mRNA accumulation was examined in different tissues by semiquantitative RT-PCR using the full-length primer. As shown in Fig. 9, both SG*rca*1 and SG*rca*2 were expressed in leaves and sepals (green tissue) but not in roots and petals (Fig. 9*A*). The calculated ratios of SG*rca1*/*rca*2 ranged from 1.862 to 2.508 in different tissues (Fig. 9*B*). To further investigate the response of RCA gene expression to photoperiod, the SG*rca*1 and SG*rca*2 mRNA accumulations were examined by qRT-PCR during the 24-h time course. For SG*rca*1, the mRNA accumulation increased significantly in the aerial leaves after the start of illumination and it reached its maximum level at 9:00 h, while that of the submerged leaves reached its maximums at 12:00 h (Fig. 10*A*). The mRNA accumulation of both the aerial and submerged leaves decreased gradually after midday and reached their minimum levels at midnight. The SG*rca*1 mRNA ratio of the aerial/submerged leaves (Fig. 10*B*) ranged from 1.34 (3:00 h) to 5.17 (6:00 h). For SG*rca*2, the similar mRNA accumulation pattern was observed in the aerial and submerged leaves (Fig. 10*C*). A delayed maximum level of SG*rca*2 mRNA accumulation occurred also in the submerged leaves. The SG*rca*2 mRNA ratio of the aerial/submerged leaves (Fig. 10*D*) ranged from 1.53 (3:00 h) to 4.48 (6:00 h).

Immunoblot analysis of Rubisco–RCA complex in aerial and submerged leaves: To further investigate the interaction between Rubisco and RCA, the Rubisco-RCA complex in leaf extracts was isolated using Rubisco antibody, and then it was probed with RCA antibody (Fig. 11*A*). Both 43 and 31 kDa RCA isoforms were detected in Rubisco-RCA complex, indicating that both two isoforms could participated in the activation of Rubisco. Interestingly, the relative abundance of the 43 and 31 kDa RCA isoforms in the Rubisco-RCA complex differed between the aerial and submerged leaves. The densitometric analysis of protein bands (Fig. 11*B*) showed that the 43/41 kDa RCA ratio in complex was 1.825 ± 0.237 ($n = 3$) in the aerial leaves, while that of the submerged leaves was 0.458 ± 0.047 ($n = 3$). The ratio of two isoform suggested that the 43 kDa RCA was the dominant isoform in Rubisco-RCA complex of the aerial leaves, while higher amount of the 31 kDa compared to the 43 kDa isoform was detected in the submerged leaves.

Discussion

Alternative mRNA splicing amplifies genetic diversity by producing two or more forms of a protein from a single gene. Alternative splicing at 3'-end of RCA coding gene was reported in *Arabidopsis* (Werneke *et al.* 1989), spinach (Werneke *et al.* 1989), barley (Rundle and Zielinski 1991), and rice (To *et al.* 1999, Zhang and Komatsu 2000). This kind of alternative slicing results in two RCA polypeptides that only differ in C-terminal end

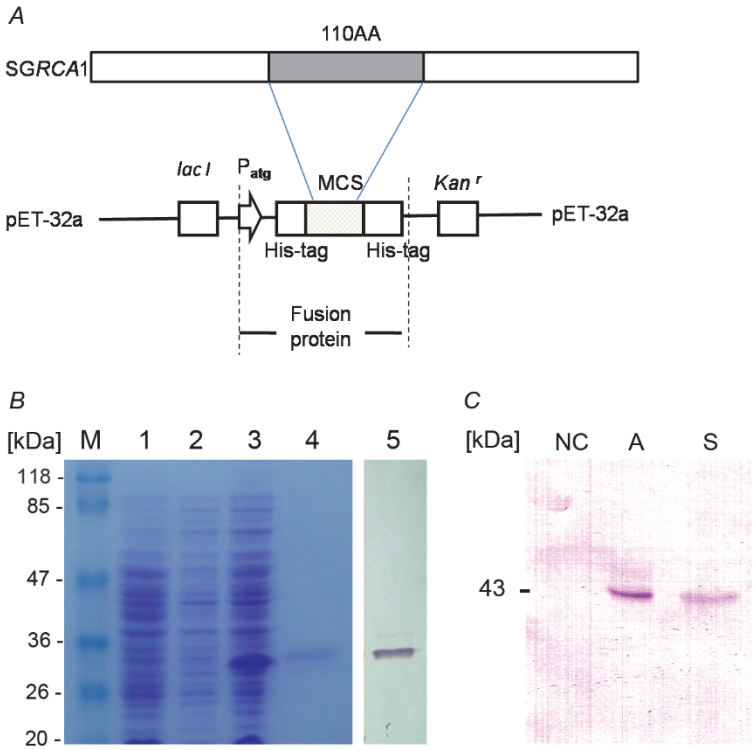

Fig. 8. Identification of the 31 kDa isoform of RCA in *Sagittaria graminea*. *A*: Schematic structure of the fusion protein pET-32a-110AA. A 330 bp DNA fragment encoding the 110 AA missing in SG*rca*2 was cloned into multiple clone site (MCS) of *Escherichia coli* expression vector pET-32a. *B*: Identification of the fusion protein pET-32a-110AA. Equal amount of lysates of recombinant bacteria (*lane 2*), IPTG induced recombinant bacteria (*lane 3*) and purified pET-32a-110AA (*lane 4*) were separated by SDS-PAGE, while lysates of *E. coli* BL21 strain with pET-32a (*lane 1*) and protein marker (*lane M*) as controls. Purified pET-32a-110AA peptide was further transferred to a PVDF membrane. Blots were probed with antibody to His tag (*lane 5*) and visualized using alkaline phosphatase conjugated to a secondary antibody. *C*: Immunoblot analysis of *S. graminea* RCA using antibody against pET-32a-110AA fusion protein. Leaf tissues from aerial (A) or submerged (S) leaf were extracted in buffer, and the RCA proteins in each crude extract was immunopurified using RCA specific monoclonal antibody, followed by Western blot analysis with antibody against 110-AA fusion peptide as described in materials and methods. Negative control sample (NC) were isolated with irrelevant antibody (anti-6 × His taq) instead of RCA antibodies.

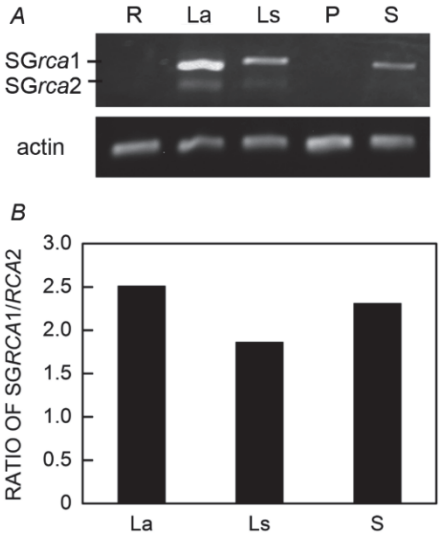

Fig. 9. RT-PCR analysis of SG*rca*1 and SG*rca*2 expression activity in different plant tissues. *A*: RT-PCR analysis was performed with actin as a control. The amplification products were separated on a 2% agarose gel. R – root; La – aerial leaf; Ls – submerged leaf; P – petal; S – sepal. *B*: The densitometric analysis of bands was performed with the *Quantity One* software, and the calculated ratios of SG*rca*1/*rca*2 from different tissues were shown.

of the enzyme. In this research, we reported a novel alternative splicing manner of RCA coding gene in the aquatic species, *S. graminea*. Two cloned cDNAs (SG*rca*1 and SG*rca*2) possessed the identical 5'- and 3'-untranslated region and only differed in the middle of the coding region by the presence or absence of the 330-bp sequence (Fig. 1), indicating that both cDNAs represented mRNA transcribed from the common gene. Gene structure analysis revealed that there were three exons and two introns in the genomic DNA clone of SG*rca*, and the alternative splicing of the 330-bp exon was located between the 3'-end of exon 2 and the 5'-end of exon 3 (Fig. 3). According to multiple sequence alignment, this novel alternative splicing pattern produced two mRNAs, both encoding β isoform of RCA (Fig. 5). This was different from four reported terrestrial species, in which the alternative splicing at 3'-end of mRNA resulted in two different isoforms belonging to α or β isoform, respectively (Werneke *et al*. 1989, Rundle and Zielinski 1991, To *et al*. 1999, Zhang and Komatsu 2000).

Higher plants usually express one or two RCA proteins with a molecular mass ranging from 41 to 47 kDa (Portis 2003). Interestingly, our results showed that two RCA polypeptides, one about 43 kDa and the other about 31 kDa, were detected by RCA specific antibody in both the aerial and submerged *S. graminea* leaves (Fig. 7*A*). These two RCA proteins were consistent in their molecular mass with the deduced mature polypeptides encoded by SG*rca*1 and SG*rca*2 cDNA clones, suggesting that they might be the translation products of those two cDNA clones. A recent study on RCA protein structure revealed that the N terminal of tobacco RCA was flexibly attached (Stotz *et al*. 2011). This lead to a question whether the 31 kDa isoform was the proteolytic product of the 43 kDa isoform. Our result using polyclonal antibody against the 110 AA, which was absent in the SG*rca*2 encoding

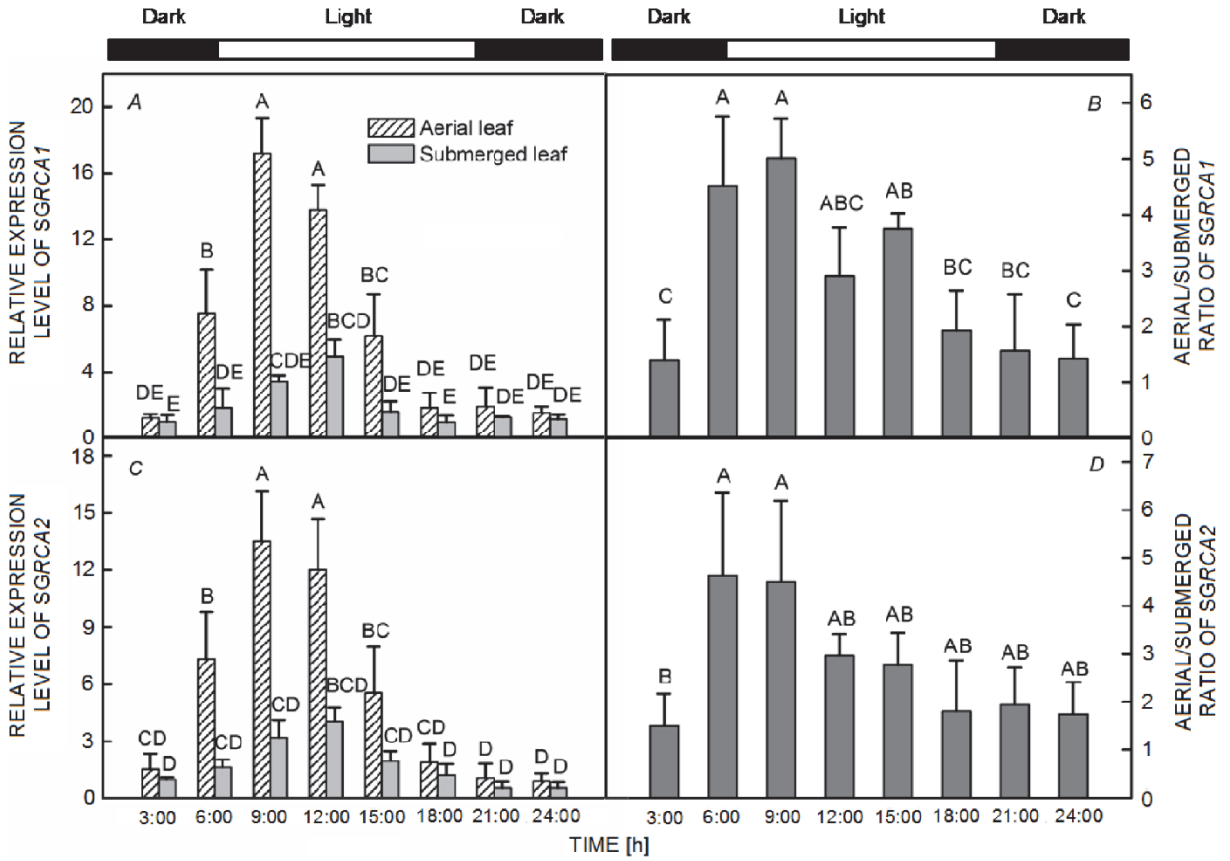

Fig. 10. qRT-PCR analysis of SG*rca*1 and SG*rca*2 mRNA levels in aerial and submerged leaves. (*A*) SG*rca*1. (*B*) Aerial/submerged ratio of SG*rca*1. (*C*) SG*rca*2. (*D*) Aerial/submerged ratio of SG*rca*2. Symbols marked with *the same letters* were not significantly different (p<0.05) for time course comparisons for different samples. The results presented are the means ± SD of 3–5 individual plants.

protein, gave evidence that the observed 31 kDa RCA protein did not contain the 110 AA (Fig. 8*C*). Since the 110 AA was located in the middle of ORF, it is impossible that the proteolytic product of the 43 kDa form without this 110 AA peptide could possess the molecular mass exceeding 20 kDa. Hence, this result demonstrated the 31 kDa RCA protein was not the proteolytic product of the 43 kDa form, but it should be encoded by SG*rca*2. Taken together, the results of mRNA accumulation (Fig. 2) and protein expression (Fig. 7) suggested both the alternative splicing products of SG*rca*1 and SG*rca*2 were expressed in *S. graminea* leaves.

In plants, such as spinach (Werneke *et al*. 1988), *Arabidopsis* (Werneke *et al*. 1988), barley (Rundle and Zielinski 1991), and rice (To *et al*. 1999, Zhang and Komatsu 2000), alternative splicing of one RCA pre-mRNA results in two isoforms of RCA (α and β isoform) differing only at the C-terminus. Although both the α- and β-isoform are capable of promoting Rubisco activation, they differ markedly in their enzyme activity (Shen *et al*. 1991). Experiments examining the reduction and oxidation of the native proteins and mixtures of the recombinant isoforms indicated that the redox changes in the larger isoform can alter the activity of the smaller isoform, through an inhibitory role of C-extension in ATP hydrolysis (Zhang and Portis 1999, Zhang *et al*. 2002, Wang and Portis 2006). In aquatic plant, *S. graminea*, the alternative splicing of RCA mRNA resulted in two protein forms which all belongs to β isoform. RCA functions as a chaperone with a classical AAA+ module that mediates Rubisco remodeling (Neuwald *et al*. 1999, Portis 2003). Bioinformatics and phylogenetic analysis showed that the 43 kDa protein encoded by SG*rca*1 had a high homology with RCA protein from other plants (75–82%) and possessed conserved motifs associated with ATPase activity and activase activity (Fig. 5), indicating that it should have similar functions as the RCA β isoform from other plants. However, the 31 kDa protein encoded by SG*rca*2 had 110 AA missing in the conserved pore loop motif concerning ATPase activity (Fig. 5), which suggested that its ATPase activity might be lost or it might have altered functions. In addition, the detection of both 43 and 31 kDa RCA isoform in Rubisco-RCA complex (Fig. 11) implied both two forms were associated with the interaction between Rubisco and RCA. *In vitro* experiments have shown that increased self-association of activase increases its activity, which is typical for many AAA proteins that typically function in an oligomeric ring structure

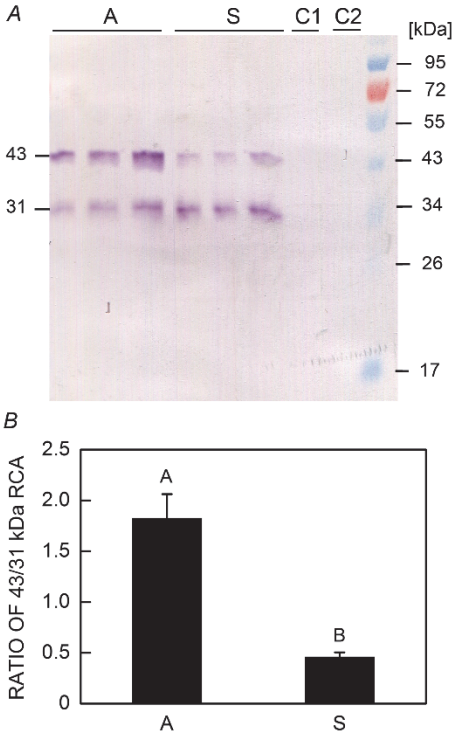

Fig. 11. Immunoblot analysis of RCA proteins in the Rubisco-RCA complex from different leaf type. *A*: Rubisco-RCA complexes in leaf extracts of aerial (A) or submerged (S) leaf were isolated by co-immunoprecipitation using monoclonal antibody to Rubisco. The eluted complex was separated by SDS-PAGE, transferred to a PVDF membrane, then probed with monoclonal antibody to rice RCA and visualized using alkaline phosphatase conjugated to a secondary antibody. Aerial (C1) or submerged (C2) leaf extracts isolated with irrelevant antibody (anti-6 × His taq) instead of Rubisco antibody were used as negative control. *B*: The densitometric analysis of protein bands was performed with *Quantity One* software, and the calculated ratios of SG*rca*1/*rca*2 from different tissues were shown in *B*. Symbols marked with *the same letters* were not significantly different ($p<0.05$) for different samples. The results presented are the means ± SD ($n = 3$).

(Salvucci 1992, Wang *et al*. 1993, Lilley and Portis 1997). A recent study on crystal structure of tobacco RCA demonstrates that RCA functions as a hexamer (Stotz *et al*. 2011). Hence, it is possible that the 31 kDa isoform participates in the formation of RCA hexamer before interacting with Rubisco, because it still possesses the conserved residues concerning RCA subunit interface and the critical residues associated with Rubisco binding (Fig. 5).

Green-tissues-specific expression of RCA genes are reported in many species (Watillon *et al*. 1993, Liu *et al*. 1996, Zhang and Komatsu 2000, Xu *et al*. 2010). Our results in aquatic plant, *S. graminea*, also showed both SG*rca*1 and SG*rca*2 were expressed only in leaves and sepals, and the two transcripts had the similar ratio in different tissues (Fig. 9*B*). The gene expression analysis of the two transcripts from the aerial and submerged leaves showed during the 24-h time course that the accumulations of SG*rca*1 and SG*rca*2 mRNA were regulated by light, which was consistent with the studies in other species (Watillon *et al*. 1993, Liu *et al*. 1996, To *et al*. 1999, Law and Crafts-Brandner 2001, Ayala-Ochoa *et al*. 2004, Xu *et al*. 2010). The similar accumulation patterns of SG*rca*1 and SG*rca*2 mRNA indicated the two alternative splicing products kept a relative balance during the photoperiod. However, in terms of different leaf types, the mRNA accumulation level of the two transcripts significantly increased in the aerial leaves than in the submerged leaves (Fig. 10*B*,*D*), suggesting that the total RCA gene expression was inhibited by the submerged environment at the transcriptional level. Furthermore, the submerged leaves reached their maximum of both SG*rca*1 and SG*rca*2 mRNA accumulation 3 h later than that of the aerial leaves during a 24-h photoperiod (Fig. 10*A*,*C*). The delayed appearance of the maximum value and the obvious inhibition of mRNA accumulation demonstrated that the submerged environment had the significantly inhibiting effect on the RCA gene expression. Studies of several heterophyllous aquatic plants have shown that the aerial leaves often exhibited higher photosynthetic capability than the submerged leaves (Nekrasova *et al*. 1998, Snir *et al*. 2006, Hyldgaard and Brix 2011). Hence, the unequally RCA mRNA accumulation between the aerial and submerged leaves of *S. graminea* could just meet the different demands of photosynthetic capability in different leaf types. At the protein level, the 43 kDa RCA encoded by SG*rca*1 was the dominant form in the aerial leaves, which agreed with its mRNA accumulation, while a relatively higher amount of the 31 kDa RCA form, encoded by SG*rca*2, was observed in the submerged leaves (Fig. 7). The inconsistency between SG*rca*2 mRNA and protein accumulation suggested that the 31 kDa isoform might undergo a post-transcriptional regulation. Considering the incompleteness of pore loop motif in the 31 kDa isoform, we speculated that this isoform might function as a negative regulator. The formation of low-active or inactive RCA-self oligomer in the submerged leaf can save the ATP consumption of RCA in the submerged condition.

In summary, the data presented here demonstrated the existence of the novel alternative splicing in aquatic plant species, *S. graminea*. The protein expression pattern of the two RCA splicing variants and their molecular characteristics imply that they might have altered functions. Our results of RCA mRNA accumulation and protein immunoblot suggested also that the RCA gene expression was regulated by the aerial or submerged environment at both the transcriptional and post-transcriptional levels, which provides new insight into photosynthesis of the heterophyllous aquatic plant *S. graminea*.

References

Ayala-Ochoa, A., Vargas-Suárez, M., Loza-Tavera, H. *et al*.: In maize, two distinct ribulose 1,5-bisphosphate carboxylase/ oxygenase activase transcripts have different day/night patterns of expression. – Biochimie **86**: 439-449, 2004.

Bradford, M.M .: A rapid and sensitive method for the quantitation of microgram quantities of protein utilizing the principle of protein-dye binding. – Anal. Biochem. **72**: 248-254, 1976.

Crafts-Brandner, S.J., Salvucci, M.E.: Rubisco activase constrains the photosynthetic potential of leaves at high temperature and CO_2. – P. Natl. Acad. Sci. USA **97**: 13430-13435, 2000.

Crafts-Brandner, S.J., van de Loo, F.J., Salvucci, M.E.: The two forms of ribulose-1,5-bisphosphate carboxylase/oxygenase activase differ in sensitivity to elevated temperature. – Plant Physiol. **114**: 439-444, 1997.

de Jiménez, E.S, Medrano, L., Martínez-Barajas, E.: Rubisco activase, a possible new member of the molecular chaperone family. – Biochemistry **34**: 2826-2831, 1995.

Eckardt, N.A., Snyder, G.W., Portis, A.R., Jr, Ogren, W.L.: Growth and photosynthesis under high and low irradiance of Arabidopsis thaliana antisense mutants with reduced ribulose-1,5-bisphosphate carboxylase/oxygenase activase content. – Plant Physiol. **113**: 575-586, 1997.

He, Z.L., von Caemmerer, S., Hudson, G.S., Price, G.D., Badger, M.R., Andrews, T.J.: Ribulose-1,5-bisphosphate carboxylase/ oxygenase activase deficiency delays senescence of ribulose-1,5-bisphosphate carboxylase/oxygenase but progressively impairs its catalysis during tobacco leaf development. – Plant Physiol. **115**: 1569-1580, 1997.

Hyldgaard, B., Brix, H.: Plasticity in carbon acquisition of the heterophyllous *Luronium natans*: An endangered freshwater species in Europe. – Aquat. Bot. **94**: 127-133, 2011.

Law, R.D., Crafts-Brandner, S.J.: High temperature stress increases the expression of wheat leaf ribulose-1,5-bisphosphate carboxylase/oxygenase activase protein. – Arch. Biochem. Biophys. **386**: 261-267, 2001.

Lilley, R.M., Portis, A.R.: ATP hydrolysis activity and polymerization state of ribulose-1,5-bisphosphate carboxylase oxygenase activase. (Do the effects of Mg^{2+}, K^+, and activase concentrations indicate a functional similarity to actin?) – Plant Physiol. **114**: 605-613, 1997.

Liu, Z.R., Taub, C.C., McClung, C.R.: Identification of an *Arabidopsis thaliana* ribulose-1,5-bisphosphate carboxylase/ oxygenase activase (RCA) minimal promoter regulated by light and the circadian clock. – Plant Physiol. **112**: 43-51, 1996.

Mate, C.J., Hudson, G.S., von Caemmerer, S. *et al*.: Reduction of ribulose bisphosphate carboxylase oxygenase activase levels in tobacco (*Nicotiana tabacum*) by antisense RNA reduces ribulose-bisphosphate carboxylase carbamylation and impairs photosynthesis. – Plant Physiol. **102**: 1119-1128, 1993.

Mate, C.J., von Caemmerer, S., Evans, J.R., Hudson, G.S., Andrews, T.J. The relationship between CO_2 assimilation rate, Rubisco carbamylation and Rubisco activase content in activase-deficient transgenic tobacco suggests a simple model of activase action. – Planta **198**: 604-613, 1996.

Nekrasova, G. F., Ronzhina, D. A., Korobitsina, E. B.: Photosynthetic apparatus in developing submerged, floating, and aerial leaves of hydrophytes. – Russ. J. Plant Physiol. **45**: 456-464, 1998.

Neuwald, A.F., Aravind, L., Spouge, J.L., Koonin, E.V.: AAA^+: A class of chaperone-like ATPases associated with the assembly, operation, and disassembly of protein complexes. – Genome Res. **9**: 27-43, 1999.

Pollock, S.V., Colombo, S.L., Prout, D.L.,Jr. *et al*.: Rubisco activase is required for optimal photosynthesis in the green alga *Chlamydomonas reinhardtii* in a low-CO_2 atmosphere. – Plant Physiol. **133**: 1854-1861, 2003.

Portis, A.R.,Jr.: Rubisco activase – Rubisco's catalytic chaperone. – Photosynth Res. **75**: 11-27, 2003.

Rundle, S.J., Zielinski, R.E.: Organization and expression of two tandemly oriented genes encoding ribulosebisphosphate carboxylase/oxygenase activase in barley. – J. Biol. Chem. **266**: 4677-4685, 1991.

Salvucci, M.E.: Subunit interactions of Rubisco activase: Polyethylene glycol promotes self-association, stimulates ATPase and activation activities, and enhances interactions with Rubisco. – Arch. Biochem. Biophys. **298**: 688-696, 1992.

Salvucci, M.E., Portis, A.R., Ogren, W.L.: A soluble chloroplast protein catalyzes ribulosebisphosphate carboxylase /oxygenase activation in vivo. – Photosynth Res. **7**: 193-201, 1985.

Salvucci, M.E., Portis, A.R.,Jr, Ogren, W.L.: Light and CO_2 response of ribulose-1,5-bisphosphate carboxylase/oxygenase activation in *Arabidopsis* leaves. – Plant Physiol. **80**: 655-659, 1986.

Salvucci, M.E., van de Loo, F.J., Stecher, D.: Two isoforms of Rubisco activase in cotton, the products of separate genes not alternative splicing. – Planta **216**: 736-744, 2003.

Salvucci, M.E., Werneke, J.M., Ogren, W.L., Portis, A.R., Jr.: Purification and species distribution of Rubisco activase. – Plant Physiol. **84**: 930-936, 1987.

Shen, J.B., Orozco, E.M., Ogren, W.L.: Expression of the two isoforms of spinach Rubisco activase and essentiality of the conserved lysine in the consensus nucleotide-binding domain. – J. Biol. Chem. **266**: 8963-8968, 1991.

Snir, A., Gurevitz, M., Marcus, Y.: Alterations in Rubisco activity and in stomatal behavior induce a daily rhythm in photosynthesis of aerial leaves in the amphibious-plant *Nuphar lutea*. – Photosynth. Res. **90**: 233-242, 2006.

Somerville, C.R., Portis, A.R.,Jr., Ogren, W.L.: A mutant of *Arabidopsis thaliana* which lacks activation of RuBP carboxylase *in vivo*. – Plant Physiol. **70**: 381-387, 1982.

Stotz, M., Mueller-Cajar, O., Ciniawsky, S., Wendler, P., Hartl, F.U., Bracher, A., Hayer-Hartl, M.: Structure of green-type Rubisco activase from tobacco. – Nat. Struct. Mol. Biol. **18**: 1366-1378, 2011.

To, K.Y., Suen, D.F., Chen, S.C.G.: Molecular characterization of ribulose-1,5-bisphosphate carboxylase/oxygenase activase in rice leaves. – Planta **209**: 66-76, 1999.

von Caemmerer, S., Hendrickson, L., Quinn, V. *et al*.: Reductions of Rubisco activase by antisense RNA in the C_4 plant *Flaveria bidentis* reduces Rubisco carbamylation and leaf photosynthesis. – Plant Physiol. **137**: 747-755, 2005.

Wang, D., Lu, Q., Li, X.F., Jiang, Q.S., Jiang, D.A.: Relationship between Rubisco activase isoform levels and photosynthetic rate in different leaf positions of rice plant. – Photosynthetica **47**: 621-629, 2009.

Wang, D., Li, X.F., Zhou, Z.J., Feng, X.P., Yang, W.J., Jiang, D.A.: Two Rubisco activase isoforms may play different roles in photosynthetic heat acclimation in the rice plant. – Physiol. Plantarum **139**: 55-67, 2010.

Wang, D., Portis, A.R., Jr.: Increased sensitivity of oxidized large

isoform of ribulose-1,5-bisphosphate carboxylase/oxygenase (Rubisco) activase to ADP inhibition is due to an interaction between its carboxyl extension and nucleotide-binding pocket. – J. Biol. Chem. **281**: 25241-25249, 2006.

Wang, Z.Y., Ramage, R.T., Portis, A.R.: Mg^{2+} and ATP or adenosine 5'-[γ-thio]-triphosphate (ATPγS) enhances intrinsic fluorescence and induces aggregation which increases the activity of spinach Rubisco activase. — Biochim. Biophys. Acta **1202**: 47-55, 1993.

Watillon, B., Kettmann, R., Boxus, P., Burny, A.: Developmental and circadian pattern of rubisco activase mRNA accumulation in apple plants. – Plant Mol. Biol. **23**: 501-509, 1993.

Werneke, J.M., Chatfield, J.M., Ogren, W.L.: Alternative mRNA splicing generates the two ribulose bisphosphate carboxylase/oxygenase activase polypeptides in spinach and *Arabidopsis*. – Plant Cell **1**: 815-825, 1989.

Werneke, J.M., Zielinski, R.E., Ogren, W.L.: Structure and expression of spinach leaf cDNA encoding ribulose bisphosphate carboxylase/oxygenase activase. — P. Natl. Acad. Sci. USA **85**: 787-791, 1988.

Xu, K., He, B., Zhou, S., Li, Y., Zhang, Y.: Cloning and characterization of the Rubisco activase gene from *Ipomoea batatas* (L.) Lam. – Mol. Biol. Rep. **37**: 661-668, 2010.

Yamori, W., Masumoto, C., Fukayama, H., Makino, A.: Rubisco activase is a key regulator of non-steady-state photosynthesis at any leaf temperature and, to a lesser extent, of steady-state photosynthesis at high temperature. – Plant J. **71**: 871-880, 2012.

Zhang, N., Kallis, R.P., Ewy, R.G., Portis, A.R., Jr.: Light modulation of Rubisco in *Arabidopsis* requires a capacity for redox regulation of the larger Rubisco activase isoform. – P. Natl. Acad. Sci. USA **99**: 3330-3334, 2002.

Zhang, N., Portis, A.R., Jr.: Mechanism of light regulation of Rubisco: a specific role for the larger Rubisco activase isoform involving reductive activation by thioredoxin-f. – P. Natl. Acad. Sci. USA **96**: 9438-9443, 1999.

Zhang, Z.L., Komatsu, S.: Molecular cloning and characterization of cDNAs encoding two isoforms of ribulose-1,5-bisphosphate carboxylase/oxygenase activase in rice (*Oryza sativa* L.). – J. Biochem. **128**: 383-389, 2000.